Microvascular patterning is controlled by fine-tuning the Akt signal

Jing Fang Sun*, Thuy Phung*, Ichiro Shiojima†, Terri Felske*, J. Nalinee Upalakalin*, Dian Feng*, Tad Kornaga*, Talia Dor*, Ann M. Dvorak*, Kenneth Walsh†, and Laura E. Benjamin*‡

*Beth Israel Deaconess Medical Center, Harvard Medical School, Boston, MA 02215; and †Boston University, Boston, MA 02215

Edited by Judah Folkman, Harvard Medical School, Boston, MA, and approved November 17, 2004 (received for review May 11, 2004)

We investigated the functions of Akt during vascular development and remodeling by using an inducible endothelial cell-specific driver of the dominant-active myrAkt. We found that sustained signaling in response to overexpression of myrAkt led to embryonic lethality, edema, and vascular malformations. In addition to the morphological malformations, the vascular phenotype was consistent with a failure in remodeling, such that the normal patterning and vessel hierarchy was disturbed. Examination of the well studied retinal vasculature during the remodeling phases revealed that transient expression of myrAkt was capable of altering the normal response to oxygen-induced remodeling without causing vascular malformations. These findings suggest that physiological levels of Akt signaling modulated microvascular remodeling and support the hypothesis that, although Akt may be required for vascular growth and homeostasis, appropriate down-regulation is also an essential aspect of normal vascular patterning.

Akt/PKB | angiogenesis | retina

Endothelial cell survival and apoptosis have been studied extensively with respect to micro- and macrovascular disease in diabetes, cardiovascular disease, sepsis, and after transplant surgery (1). As a desired effect of therapy, endothelial cell apoptosis has been explored in response to antiangiogenic treatments for cancer (2). Less attention has been paid to the control of endothelial cell apoptosis during development, although it has been proposed to explain the overall decrease in microvascular density associated with microvascular remodeling.

Much of the classical work on microvascular remodeling has been done in the developing retina because of its planar architecture and accessibility, because the expansion and remodeling of this vascular bed is postnatal. A series of elegant studies have clearly established VEGF-A as a driver of vascular expansion in this organ in both development (3, 4) and pathological neovascularization (5–7) as well as a regulator of endothelial cell survival during the remodeling process (8). In the retina, VEGF-A is provided largely by the astrocytes, which enter the retina through the optic disk and spread radially toward the periphery in advance of blood vessel formation (3, 9). The astrocytes are exquisitely sensitive to oxygen levels and strongly induce VEGF-A in hypoxic regions of the retina (10, 11). As the astrocytes and expand radially across the retina, they attract the endothelium to follow and lay a scaffold on which blood vessels form, in part due to the molecular attraction of VEGFR-2 expressed on endothelial cell filopodia with sequestered VEGF on the astrocyte surface (9). Once the new blood vessels bring oxygen to the formerly hypoxic regions of the retina, local VEGF-A levels drop. These events initiate the remodeling process where vessel regression is coordinated with pericyte-induced stabilization (12, 13). This coordination of oxygen-induced VEGF-A reduction and pericyte stabilization has led to the hypothesis that the balance in survival signaling determines the final outcome of microvessel remodeling.

Both Fas-mediated apoptosis and VEGF-mediated survival signaling have been implicated in the control of microvascular remodeling (8, 14). Survival signaling via the Akt/PKB serine threonine kinase is activated in endothelial cells downstream of endothelial cell growth factors such as VEGF-A and angiopoietin-1, cell–cell contacts, and shear stress, and has been implicated in controlling vascular growth and homeostasis (15). Null animals for the three Akt genes, Akt1, -2, and -3, have not provided much insight into the normal role of Akt in endothelial cells, perhaps because of redundancy or the pleiotropic nature of these proteins (16). As an alternative to these loss-of-function approaches, we have explored the role of dominant-active myrAkt signaling during microvascular remodeling and show that transient signaling impacts normal physiological microvascular development, whereas sustained Akt signaling causes microvascular malformations reminiscent of developmental vascular anomalies.

Materials and Methods

Transgenic Mice. The VE-cadherin promoter was cloned upstream of the tetracycline-regulated transcriptional activator (tTA) gene by using published sequences (38). The primers used were: forward, 5′-AGCCTAGGTGAGCGTCCCCT, and reverse, 5′-TGTCCAGGGCCGAGTTTGTG. Genotyping for the tTA gene was done by PCR using the primer pair: forward, 5′-gacgccttagccattgagat and reverse 5′-CAGTAGTAGGTGTTTCCCTTTCTT. TET:myrAkt mice were constructed by using full-length Akt1 with a c-Src myristoylation sequence and hemagglutinin tag added to the N terminus. Four founder lines of VE-cadherin:tTA and two from TET:myrAkt were tested and performed similarly. Genotyping for the Akt1 transgene was done by PCR using the following primer pair: forward, 5′-TGGAGGACAACGACTACGG, and reverse, 5′-ACACGATGTTGGCAAAGAA. For the analysis presented above the D5 line (VE-cadherin:tTA) and K8 line (TET:myrAkt) were used. To suppress myrAkt expression in embryos and neonates, 1.5 mg/ml tetracycline with 5% sucrose was given to pregnant and lactating females in their drinking water.

Whole-Mount Immunofluorescence and Immunohistochemistry. For whole-mount preparations, the eyes were fixed with 10% formalin at 4°C overnight. Eyes were enucleated, the cornea, lens, and sclera were removed to expose the retinas, and hyaloid vessels removed when necessary. After washing with PBS for 15 min three times and blocking with PBS containing 0.5% Triton X-100, 0.02% azide, PBS, and 10% goat serum for 1–3 h, the eyes were incubated with shaking at 4°C overnight with *Bandeiraea simplicifolia* BS-1 Isolectin (LEC)-TRIC (Sigma) in a PBS buffer containing 0.5% Triton X-100, 0.02% azide, and 10% goat serum. Retinas were washed four to five times for 1 h each with

This paper was submitted directly (Track II) to the PNAS office.

Freely available online through the PNAS open access option.

Abbreviations: tTA, tetracycline-regulated transcriptional activator; PlGF, placenta growth factor; P*n*, postnatal day *n*; E*n*, embryonic day *n*; PARP, poly(ADP ribose) polymerase; CFZ, capillary-free zone.

‡To whom correspondence should be addressed. E-mail: lbenjami@bidmc.harvard.edu.

www.pnas.org/cgi/doi/10.1073/pnas.0403198102

Table 1. The primer sequences for the target genes

Target genes	Forward primer	Reverse primer
mVE-Cadherin	5′-GGCCCTGGACAGACTGCA-3′	5′-CCTTCGTGGAGGAGCTGATC-3′
mβ-actin	5′-AACCGTGAAAAGATGACCCAGAT-3′	5′-CACAGCCTGGATGGCTACGT-3′

PBS, and four incisions were used to flatten and mount the retina under coverslips. The flat-mounted retinas were viewed with conventional fluorescence microscopy. Images are captured by using a Leica DC200 digital camera and software. Perfusion, when indicated, was visualized after tail-vein injection of Lectin-FITC 30 min before harvesting retinas.

Quantitation of mRNA Expression. Retinas were separated in DEPC-PBS. Total RNA was extracted by using TRIzol reagent (Invitrogen). cDNA was synthesized by TaqMan Reverse Transcription Reagents with random primers (Applied Biosystems) followed by real-time PCR in the ABI Prism 7000 Sequence Detection System (Applied Biosystems). Primers were designed by using the primer design software PRIMER EXPRESS 2.0 (Applied Biosystems). The forward and reverse primers are located in different exons. The primer sequences for the target genes are shown in Table 1. cDNA samples, prepared as in RT-PCR above, were mixed with primers and SYBR Master Mix (Applied Biosystems) in a total volume of 25 μl. PCR was conducted by using the following parameters: 95°C for 10 min, and 40 cycles at 95°C for 15 s and 60°C for 1 min. PCRs were performed in 96-well optical reaction plates (Applied Biosystems). Quantitative real-time PCR was normalized to the copies of β-actin mRNA from the same sample. Acquired data were analyzed by SEQUENCE DETECTOR software (Applied Biosystems).

Survival Assay. Subconfluent cultures of bovine retinal endothelial cells (VEC Technologies, Rensselaer, NY) incubated at 37°C with 20% O_2 and 5% CO_2 were starved overnight in serum-free MCDB-131 Complete media (VEC Technologies). $VEGF_{165}$, $VEGF_{121}$, VEGF-C, VEGF-D, placenta growth factor (PlGF), or VEGF/PlGF (R & D Systems) were added to individual culture plates for a final concentration of 50 ng/ml. Samples containing either 10% FBS in MCDB-131 or serum-free MCDB-131 were used as positive and negative controls, respectively. After the cells were treated with growth factor for 48 h, they were harvested with trypsin-EDTA, washed with PBS, fixed overnight in 70% ethanol, and then stained with propidium iodide (Sigma). Approximately 10,000 cells in each sample were analyzed by analyzed by FACS on a Becton-Dickinson FACS instrument.

Results and Discussion

Before remodeling, a clear morphological distinction between arteries and veins is not evident, as shown here in a whole-mount image of the blood vessels in the early postnatal mouse retina (Fig. 1*a*, postnatal day 3, P3). Previous studies have implicated oxygen flow through the newly formed vasculature as the initiator of remodeling. The coincidence of oxygenation and remodeling was first proposed because the earliest notable morphological change associated with remodeling is the clearing of microvessels near the arterial vessels to form the capillary-free zone (CFZ), which is indicated by a bar across the arterial vessel (Fig. 1*a*, P7). This CFZ is maintained and expanded along major branches from the arteriole. The result is a gradual reduction in the vascular density in a gradient along the arterial vessels toward the veins (Fig. 1*a*, P13). Investigators have shown that this natural process of capillary reduction can be exaggerated by placing the neonates in hyperoxia (a 75–80% oxygen chamber, rather than the 21% oxygen found in room air). Hyperoxia-induced capillary clearing is the first step in a protocol that

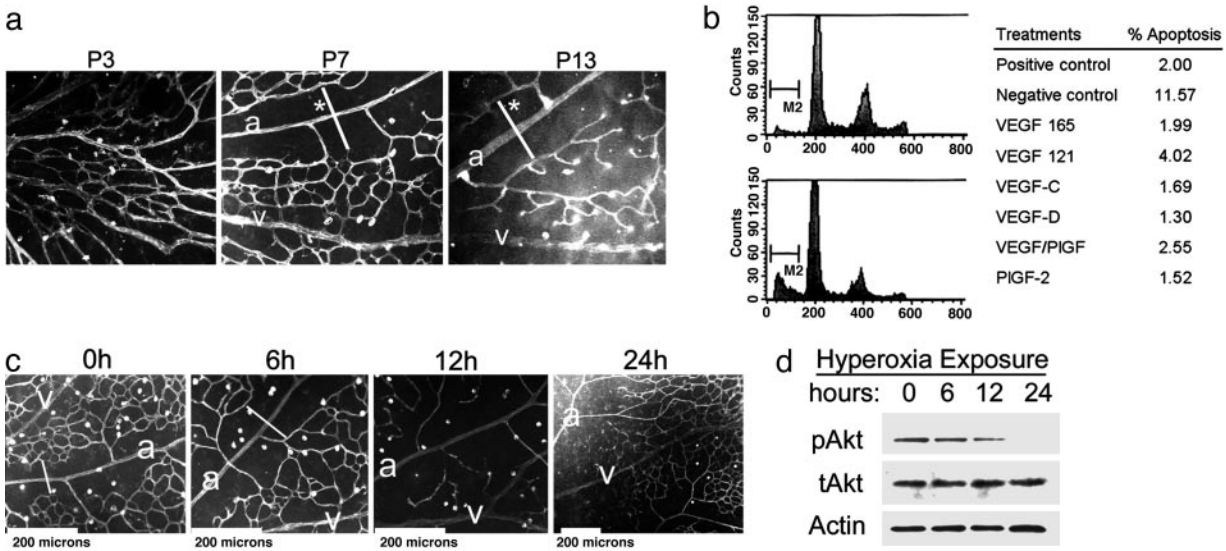

Fig. 1. Survival functions in retinal remodeling. (*a*) Microvascular remodeling during normal retinal development is shown after Lectin BS-1 (Sigma) staining to highlight the lack of vessel definition before remodeling in a P3 mouse, followed by the formation of a CFZ that defines arterial vessels by P7, and the further extension of capillary reduction from the arterial vessel toward the vein by P13 in the region closest to the optic disk, which is at the left edge of all of these images. (*b*) FACS histograms of DNA content for negative (0% FBS) and positive (10% FBS) control are shown on left, and results listed for all factors tested are shown on right. (*c*) The acceleration of capillary reduction is achieved by hyperoxia exposure. The CFZ doubles in size from 0 to 6 h, and by 24 h total clearing of microvessels from artery to vein is observed in a circular region surrounding the optic disk. The image for 24 h is half the magnification of the rest to show distance of clearing. (*d*) This exaggerated formation of a CFZ is coincident with decreased Akt phosphorylation as marked by Western blot for pAkt (BD Pharmingen). Total Akt (Santa Cruz Biotechnology) and actin (Sigma) serve as protein loading controls. a, arterial vessel; v, vein; *, CFZ.

mimics the human disease retinopathy of prematurity (17, 18). Once remodeling is complete, mature vascular beds are insensitive to hyperoxia-induced regression. This excessive reduction in capillaries occurs throughout the retina. However, because of the spherical shape of the retina and the radial structure of the vessels emanating from the optic disk, the exaggerated remodeling leads to total loss of capillaries in the region nearest the optic disk, where the arterioles are closest together. Thus, we can visually assess the extent of regression by focusing on the area adjacent to the optic disk. Because VEGF-A is controlled by oxygen both at the transcriptional level and posttranscriptional level (19–21), elegant studies clearly linked this oxygen-induced microvessel regression to loss of VEGF-A survival function (8). VEGF-A is not the only growth factor that provides survival signals to endothelium, and similar results have been reported in the retina with IGF, PlGF, and PlGF/VEGF heterodimers (22–24). We tested survival function by quantifying the ability of VEGF family members to protect retinal endothelial cells from apoptosis after serum withdrawal. DNA content analysis was performed by using FACS to quantify the number of cells in each culture that undergo apoptosis. Cells in apoptosis are hypodiploid and therefore fall at channels below 200, represented by M2 on the histogram. We found that all of the growth factors significantly reduced apoptosis compared to the negative control (Fig. 1*b*). In fact, with the exception of $VEGF_{121}$, they were comparable or even better than the positive control (full media with serum). Some growth factors were similarly effective at lower concentrations (like $VEGF_{165}$), but we found 50 ng/ml to be a relatively low concentration where we could still see the effects of most endothelial growth factors.

Many *in vitro* studies have implicated the phosphatidylinositol 3-kinase/Akt pathway in the survival functions of VEGF-A and other endothelial cell cytokines (15). If Akt signaling mediates the regression that is part of retinal remodeling, one would predict that Akt signaling in retinal blood vessels should be related to oxygen exposure. To test this prediction, we placed newborn mice at P7 in 75% oxygen for increasing lengths of time. We then monitored the effects on capillary clearing near the optic disk (Fig. 1*c*) and correlated this to the levels of phosphorylated Akt in freshly isolated retinal tissue (Fig. 1*d*). Similar to the sequence of events in the natural remodeling process, the first observable alteration was an increase in the size of the CFZ after 6 h of hyperoxia. Before oxygen, the CFZ in P7 retinas was 0.10 mm, and 6 h later it had increased nearly 2-fold (0.18 mm) (Fig. 1*c*). Capillary clearing continued in this zone closest to the optic disk until it was completely cleared by 24 h. Overall microvessel reduction occurred farther from the optic disk, but microvessels still remained in peripheral regions after 24 h. Retinas were rapidly dissected away from the lens and choroid, immediately homogenized in protein lysis buffer, and Akt phosphorylation was measured by Western blot analysis (Fig. 1*d*). Although small local alterations in remodeling were visible at 6 and 12 h (e.g., the increased CFZ), the number of endothelial cells affected at this point is a small fraction of the retinal vessels and is not significant enough to be visible when whole retinal lysates are used for Akt detection. However, by 12 h, decreased levels of overall phospho-Akt levels in the whole retina were beginning to be detected, a reflection of the more widespread alterations in vessel density. Thus, loss of blood vessels in the retina was strongly correlated to overall decreased expression of phospho-Akt. The multiple published studies on this oxygen-induced regression has shown that the change in vascular survival in oxygen is due to loss of VEGF expression by reductions in hypoxia-inducible factor-mediated transcription and loss of VEGF-A mRNA stability (25). The loss of VEGF in hyperoxia could account for the loss of Akt signaling in endothelial cells. Taken together with the established literature, these data support the hypothesis that local changes in VEGF-Akt signaling mediate the survival and regression of microvessels during remodeling. However, although vascular regression is still relatively mild at 6–12 h, the loss of perfusion and increased oxygen levels may also affect the viability of other cell types in the retina, and using whole retina lysates, we cannot rule out that some of the Akt signaling that we see is from nonendothelial cell types. Nonetheless, as we show in the figures below, increased endothelial cell-specific Akt signaling during hyperoxia can reduce apoptosis measured in whole retinal lysates.

To regulate endothelial cell-specific Akt signaling, we used a binary transgenic model of myrAkt, a dominant active form, to override oxygen-mediated Akt loss in the retinal vasculature. First, we created endothelial cell-specific driver mice by cloning tTA behind the endothelial cell-specific VE-cadherin promoter. Shown in Fig. 2, expression of tTA can be monitored by mating these mice to a reporter strain that has the tetracycline-responsive promoter driving β-galactosidase expression (TET:lacZ). Fig. 2*a* shows β-galactosidase expression in the blood vessels of double transgenic mice in embryos (embryonic day 13.5, E13.5) and Fig. 2*b* shows this expression in the retinal vasculature. We demonstrated that the β-galactosidase gene is expressed exclusively in endothelial cells by costaining for anti-VEGFR-2 (Fig. 2*c*) and CD31 (data not shown). When we crossed these VE-cadherin:tTA mice with mice containing a TET:myrAkt transgene, we found that sustained expression of myrAkt resulted in an embryonic lethal phenotype that could be suppressed by providing tetracycline to the drinking water of the pregnant females. When double transgenic animals were allowed to develop in the presence of tetracycline, they were phenotypically normal, and we could induce myrAkt expression in the retinal vasculature by removing tetracycline in both adults and neonates (Fig. 2 *d* and *e*). Not only were there increased levels of hemagglutinin-tagged myrAkt in these retinas, but we could also measure increased levels of phosphorylated Akt. Reminiscent of pathological settings where the Akt signaling pathway may be chronically induced by ischemic induction of VEGF-A or other growth factors, sustained expression of myrAkt (for 7 days) led to multiple vascular malformations in mature retinas (Fig. 2*e*). The balloon-like structures that formed were shown to be perfused when lectin was administered through the tail vein (data not shown). The structure of these abnormalities suggested that, unlike glomeruloid-like structures that form in retinopathy and glioblastomas, these malformations were more similar to microaneurysms or developmental vascular anomalies. We used morphometric analysis to compare the vascular changes, in particular vascular size which was the most dramatic change in vascular structure. More than 15 vessel diameters were measured in each animal. Capillaries in wild-type control littermates with a single transgene were highly consistent (Fig. 2*f*, wt); however, the vessels in the double transgenic animals were not only significantly larger, but also much more variable (Fig. 2*f*, tg). The great variability in vascular size may reflect local variations in Akt levels. Note that these measurements were made on tissue fixed overnight, and some postfixation shrinkage has occurred, so that the micrometer values are an underestimate of the actual vessel diameter in live animals.

By using transient pulses of myrAkt, we could test our hypothesis that Akt expression in the remodeling retina mediates microvessel clearing. This assay required only 2 days of tetracycline withdrawal, and the neonates remained healthy and phenotypically normal during this period. In this assay, the morphological abnormalities associated with sustained expression were not seen. To control for possible confounding effects of tetracycline, both double transgenic animals and their littermates were maintained on tetracycline until 24 h before oxygen exposure. These animals and control littermates were then placed in 75% oxygen for an additional 24 h. Retinas were harvested for immunostaining of blood vessels and isolation of RNA and protein. Fig. 3*a* shows the clearing of capillaries near the optic disk in control and double transgenic retinas. To supplement the visual inspection of the retinas near the optic disk, we used

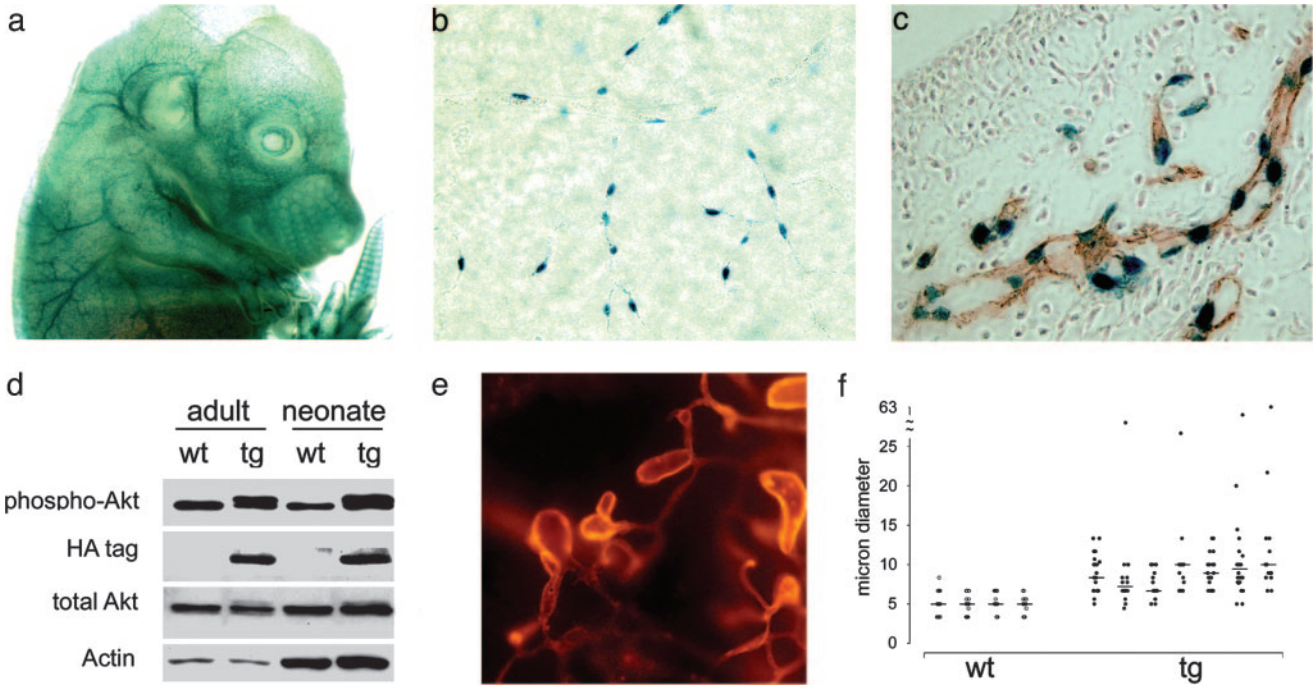

Fig. 2. Sustained endothelial cell-specific expression of myrAkt driven by VE-cadherin promoter-tTA transgenic mice induces microvascular malformations in the mature retina. VE-cadherin:tTA mice crossed to TET:lacZ mice shows β-galactosidase expression in embryonic blood vessels (E14.5) (*a*), retinal blood vessels (*b*), and costaining of β-galactosidase with anti-VEGFR-2 (*c*). (*d*) Western blot analysis of retinas from adults and neonates show transgene expression by using hemagglutinin (HA) tag (Roche Diagnostics) and increased levels of phosphorylated Akt (BD Pharmingen). (*e*) Sustained expression of myrAkt causes malformations reminiscent of microaneurysms in the retina. (*f*) Red Lectin-TRITC staining. Retinal vessel diameter from double transgenic pups (seven animals) is significantly larger than vessel diameter from control pups (four animals) after adjusting for litter effects by stratified Wilcoxon–Mann–Whitney test, $P < 0.0001$.

real-time RT-PCR to quantify the vascular burden throughout the retina. This highly quantitative measure of VE-cadherin levels was used as a relative read-out of endothelial cell numbers. Control animals had total clearing of microvessels near the optic disk and a 20-fold reduction in VE-cadherin mRNA levels throughout the retina ($n = 12$). In mice expressing myrAkt in endothelial cells, microvessel clearing near the optic disk was incomplete, and there was only a 2-fold reduction in VE-cadherin mRNA levels ($n = 10$). This result is reminiscent of what has been previously reported when VEGF-A is injected into the vitreous, further supporting our hypothesis that Akt signaling mediates the effects of VEGF-A on survival during remodeling (8). Previous investigators have implicated apoptosis in the microvessel reduction during remodeling. Therefore, we tested the hypothesis that the survival signaling function of Akt participated in the oxygen-induced remodeling by quantification of poly(ADP ribose) polymerase (PARP) cleavage. Using an antibody that recognizes both p85 and p25 cleavage products, we showed that apoptosis is increased dramatically in control retinas after hyperoxia exposure, and that myrAkt expression reduced that apoptosis (Fig. 3*b*).

We investigated whether ectopic expression of Akt during remodeling phases of other organs would result in aborted remodeling. Other vascular beds are more complicated to assess, because they do not have the advantage of spatially separate vessel formation and remodeling as the retina does. Nonetheless, some aspects of remodeling could not be assessed in the retina. For example, in addition to the overall reduction in capillaries, remodeling also consists of the concomitant establishment of a hierarchy of vessel sizes. We were unable to maintain myrAkt expression in neonates to examine this aspect of remodeling because the time course for those changes exceeds the time in which neonates remain phenotypically normal and healthy with sustained myrAkt expression. However, in embryos, the remodeling is more rapid, and we turned to another model system, the embryonic skin, which establishes a reproducible and classic arbor-like vascular tree over a period of 48 h in midgestation. We visualized this remodeling vascular bed in the embryonic flank in E12.5–14.5 stage embryos by using Tie-2:lacZ transgenic mice that express the β-galactosidase gene in endothelial cells. At E12.5, the vessels are web-like and disorganized similar to the earliest retinal blood vessels (compare Fig. 4*a* to Fig. 1*a*, P3). By E14.5, these vessels have remodeled into a classic arbor-like vasculature (Fig. 4*b*). If we allowed expression of myrAkt during this time frame and examined embryos, we could clearly see that this arbor-like pattern did not form (compare Fig. 4 *c* with *d*). Akt has other functions besides survival that are likely contributing to the embryonic phenotype, such as changes in permeability (evident by wrinkled skin), and some vessel tortuosity that may result from increased proliferation. Nonetheless, even with this caveat, we could clearly see that patterning of the major embryonic skin vessels did not occur. Rather than a graded distribution in vessel size and organized connections between branching blood vessels as we see in controls (Fig. 4*c*), vessels remained more or less of equal size without a clear hierarchical organization (Fig. 4*d*). Compared to control embryos E14.5 (Fig. 4*e*), the double transgenic littermates (Fig. 4*f*, arrowhead) contained erythrocyte-congested blood vessels. We also observed dermal edema, especially noticeable in sections because of the increased size of the connective tissue layer beneath the dermis. We found extravascular erythrocytes in some places, although we could find no evidence of apoptosis either by conventional histology or EM of endothelial cell nuclei. The EM analysis did reveal small disruptions in the endothelial cell lining with erythrocytes leaking into the surrounding matrix (Fig. 4*g*). The arrowhead in Fig. 4*g* points to an extravascular erythrocyte, and the arrow shows erythrocyte extravasation.

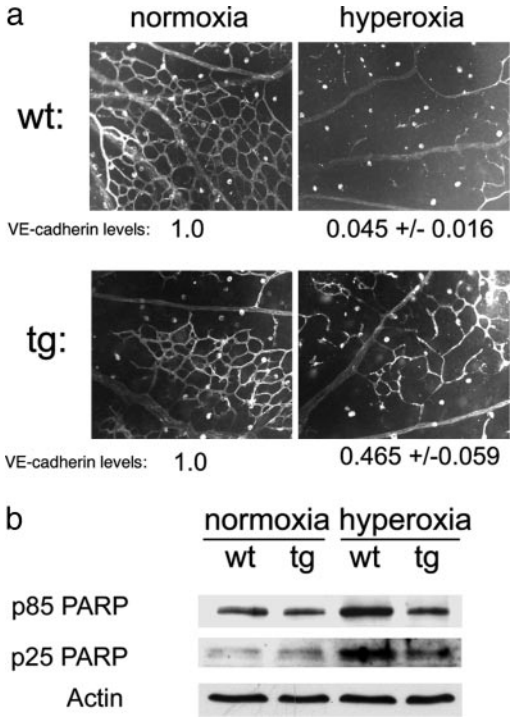

Fig. 3. Transient expression of myr-Akt impairs oxygen-induced reductions in microvessel density and apoptosis during remodeling. (*a*) Whole-mount immunohistochemistry of retinas using BS-I Lectin-TRITC on control and double transgenic P7 neonatal mice before (normoxia) and after (hyperoxia) show the block in exaggerated capillary clearing coincident with Akt induction. VE-cadherin mRNA levels were quantified by real-time RT-PCR and shown below each panel relative to normoxia control. (*b*) Western blot analysis of PARP cleavage was used to quantify apoptosis in retinas after hyperoxia with and without transgenic myrAkt expression. The PARP antibody (Biosource) recognizes the p25 and p85 cleavage products. wt, wild type; tg, double transgenic.

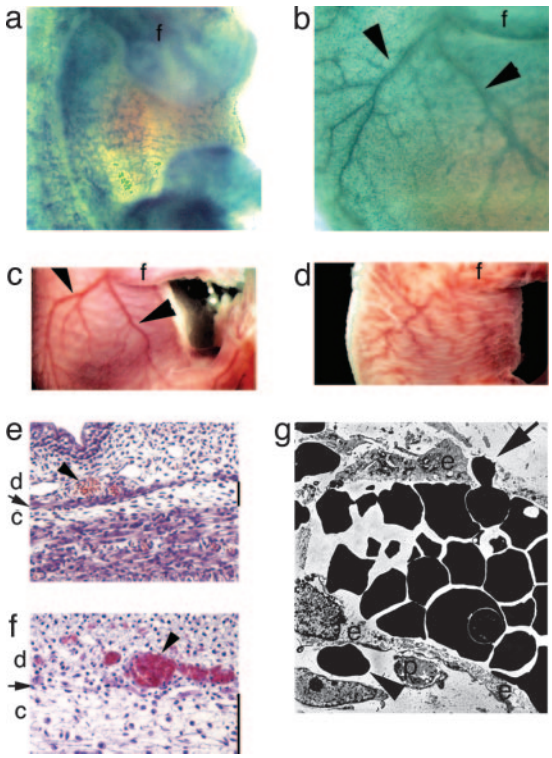

Fig. 4. Inducible myr-Akt blocks normal remodeling in embryonic skin. Tie-2:lacZ transgenic mice were used to visualize blood vessels in embryo at E12.5 (*a*) and E14.5 (*b*) to show remodeling of the immature capillary network into arbor-like vessels. Compared to the normal embryonic vasculature (*c*), in double transgenic VE-cadherin:tTA;TET:myrAkt embryos, this remodeling is abnormal and an arbor-like hierarchy does not form (*d*). (*e*) Histology of wild-type embryonic skin as a control. (*f*) Double transgenic skin shows edema in s.c. adipose tissue, disruption of the skeletal muscle layer (highlighted with an arrow), and congested and large vessels in the dermis. Note the increased size of the connective tissue layer, as indicated with a bar on the right. (d, dermis; c, connective tissue). Images are the same magnification. (*g*) Electron microscopy of double transgenic embryos reveals frank disruptions of the vessel wall and erythrocyte leakage without evidence of endothelial cell necrosis or apoptosis (e, endothelial cell; p, pericyte).

In conclusion, we have demonstrated that proper remodeling requires fine-tuning of the Akt signaling pathway. The outcome of remodeling depends on appropriate stimulation and repression of this pathway. Stimulation may be provided by soluble cytokines, such as VEGF-A, in the remodeling retina. Previous studies that demonstrate VEGF-A independence in mature vessels suggest that other stabilizing forces come into play after remodeling (13, 26). Some examples that have been described that contribute to microvessel stability include pericyte/vascular smooth muscle association. Our results show that, in addition to stimulating the Akt signaling pathway during development, it is equally important to spatially and temporally down-regulate Akt signaling. Many studies have contributed to our understanding of Akt signaling in the vasculature (15). In particular, other cytokines, such as the angiopoietins, known to be important for both stabilization and neovascularization in the retina (27, 28), also activate Akt signaling in cultured cells (29–32). However, our data show that even if they can activate this pathway *in vivo*, their endogenous levels are not sufficient to fully compensate for the loss of VEGF-A that occurs in hyperoxia.

Given the dramatic alterations that result from sustained signaling of Akt in these studies, we surmise that such pathways may play a role in vascular malformations or tumor angiogenesis, both typified by enlarged and irregular vessels. The chronic exposure to tumor secreted cytokines may result in chronic activation of Akt in tumor blood vessels, and activating mutations in endothelial cell receptor tyrosine kinases such as Tie-2 may lead to sustained signaling in genetic vascular malformations (33–35). Previous studies implicated signal transducer and activator of transcription 1 (STAT1) in these malformations that arose from Tie-2 mutations, but recent demonstrations that angiopoietin-binding Tie-2 stimulates Akt signaling and abrogation of Tie-2 function results in a block in Akt signaling suggest that Akt signaling may contribute to vascular malformations when Tie-2 is constitutively activated (29, 31, 36, 37). Most prior investigation of the Akt signaling pathway in endothelial cells has relied on sustained expression of dominant active Akt either by means of viral administration or transfection studies, and thus much of our understanding of downstream pathways arises from such settings. Our study uses inducible and endothelial cell-specific expression of myrAkt in transgenic mice to study the role of Akt signaling in vascular development. Future investigation into how downstream signaling may differ after sustained or physiological stimulation is warranted.

We thank Carole Perruzzi, Karen Balonze, Cassidy Foley, and Daniel Ghalchi for technical assistance and Shuli Li for help with the statistical analysis. This work was supported by American Heart Association grants and National Institutes of Health Grants 1 R01 HL071049 and CA109086.

1. Dimmeler, S. & Zeiher, A. M. (2000) *Circ. Res.* **87,** 434–439.
2. Liu, W., Ahmad, S. A., Reinmuth, N., Shaheen, R. M., Jung, Y. D., Fan, F. & Ellis, L. M. (2000) *Apoptosis* **5,** 323–328.
3. Stone, J., Itin, A., Alon, T., Pe'er, J., Gnessin, H., Chan-Ling, T. & Keshet, E. (1995) *J. Neurosci.* **15,** 4738–4747.
4. Provis, J. M., Leech, J., Diaz, C. M., Penfold, P. L., Stone, J. & Keshet, E. (1997) *Exp. Eye Res.* **65,** 555–568.
5. Pe'er, J., Shweiki, D., Itin, A., Hemo, I., Gnessin, H. & Keshet, E. (1995) *Lab. Invest.* **72,** 638–645.
6. Aiello, L. P. & Wong, J. S. (2000) *Kidney Int. Suppl.* **77,** S113–S119.
7. Miller, J. W. (1997) *Am. J. Pathol.* **151,** 13–23.
8. Alon, T., Hemo, I., Itin, A., Pe'er, J., Stone, J. & Keshet, E. (1995) *Nat. Med.* **1,** 1024–1028.
9. Gerhardt, H., Golding, M., Fruttiger, M., Ruhrberg, C., Lundkvist, A., Abramsson, A., Jeltsch, M., Mitchell, C., Alitalo, K., Shima, D. & Betsholtz, C. (2003) *J. Cell Biol.* **161,** 1163–1177.
10. Shweiki, D., Itin, A., Soffer, D. & Keshet, E. (1992) *Nature* **359,** 843–845.
11. Stone, J., Chan Ling, T., Pe'er, J., Itin, A., Gnessin, H. & Keshet, E. (1996) *Invest. Ophthalmol. Vis. Sci.* **37,** 290–299.
12. Orlidge, A. & D'Amore, P. A. (1987) *J. Cell Biol.* **105,** 1455–1462.
13. Benjamin, L. E., Hemo, I. & Keshet, E. (1998) *Development (Cambridge, U.K.)* **125,** 1591–1598.
14. Ishida, S., Yamashiro, K., Usui, T., Kaji, Y., Ogura, Y., Hida, T., Honda, Y., Oguchi, Y. & Adamis, A. P. (2003) *Nat. Med.* **9,** 781–788.
15. Shiojima, I. & Walsh, K. (2002) *Circ. Res.* **90,** 1243–1250.
16. Franke, T. F., Hornik, C. P., Segev, L., Shostak, G. A. & Sugimoto, C. (2003) *Oncogene* **22,** 8983–8998.
17. Pierce, E. A., Foley, E. D. & Smith, L. E. (1996) *Arch. Ophthalmol.* **114,** 1219–1228.
18. Smith, L. E., Wesolowski, E., McLellan, A., Kostyk, S. K., D'Amato, R., Sullivan, R. & D'Amore, P. A. (1994) *Invest. Ophthalmol. Vis. Sci.* **35,** 101–111.
19. Shweiki, D., Neeman, M., Itin, A. & Keshet, E. (1995) *Proc. Natl. Acad. Sci. USA* **92,** 768–772.
20. Forsythe, J. A., Jiang, B. H., Iyer, N. V., Agani, F., Leung, S. W., Koos, R. D. & Semenza, G. L. (1996) *Mol. Cell. Biol.* **16,** 4604–4613.
21. Stein, I., Itin, A., Einat, P., Skaliter, R., Grossman, Z. & Keshet, E. (1998) *Mol. Cell. Biol.* **18,** 3112–3119.
22. Smith, L. E., Shen, W., Perruzzi, C., Soker, S., Kinose, F., Xu, X., Robinson, G., Driver, S., Bischoff, J., Zhang, B., *et al.* (1999) *Nat. Med.* **5,** 1390–1395.
23. Upalakalin, J. N., Hemo, I., Dehio, C., Keshet, E. & Benjamin, L. E. (2002) *Cold Spring Harbor Symp. Quant. Biol.* **67,** 181–187.
24. Shih, S. C., Ju, M., Liu, N. & Smith, L. E. (2003) *J. Clin. Invest.* **112,** 50–57.
25. Dor, Y., Porat, R. & Keshet, E. (2001) *Am. J. Physiol.* **280,** C1367–C1374.
26. Benjamin, L. E., Golijanin, D., Itin, A., Pode, D. & Keshet, E. (1999) *J. Clin. Invest.* **103,** 159–165.
27. Hackett, S. F., Wiegand, S., Yancopoulos, G. & Campochiaro, P. A. (2002) *J. Cell Physiol.* **192,** 182–187.
28. Gale, N., Thurston, G., Hackett, S., Renard, R., Wang, Q., McClain, J., Martin, C., Witte, C., Witte, M., Jackson, D., *et al.* (2002) *Dev. Cell* **3,** 411–423.
29. Fujikawa, K., de Aos Scherpenseel, I., Jain, S. K., Presman, E., Christensen, R. A. & Varticovski, L. (1999) *Exp. Cell Res.* **253,** 663–672.
30. Papapetropoulos, A., Fulton, D., Mahboubi, K., Kalb, R. G., O'Connor, D. S., Li, F., Altieri, D. C. & Sessa, W. C. (2000) *J. Biol. Chem.* **275,** 9102–9105.
31. Kim, I., Kim, H. G., So, J. N., Kim, J. H., Kwak, H. J. & Koh, G. Y. (2000) *Circ. Res.* **86,** 24–29.
32. Kim, I., Kim, J. H., Moon, S. O., Kwak, H. J., Kim, N. G. & Koh, G. Y. (2000) *Oncogene* **19,** 4549–4552.
33. Hatva, E., Jaaskelainen, J., Hirvonen, H., Alitalo, K. & Haltia, M. (1996) *J. Neuropathol. Exp. Neurol.* **55,** 1124–1133.
34. Hashimoto, T., Lam, T., Boudreau, N. J., Bollen, A. W., Lawton, M. T. & Young, W. L. (2001) *Circ. Res.* **89,** 111–113.
35. Vikkula, M., Boon, L. M., Carraway, K. L., III, Calvert, J. T., Diamonti, A. J., Goumnerov, B., Pasyk, K. A., Marchuk, D. A., Warman, M. L., Cantley, L. C., *et al.* (1996) *Cell* **87,** 1181–1190.
36. Korpelainen, E. I., Karkkainen, M., Gunji, Y., Vikkula, M. & Alitalo, K. (1999) *Oncogene* **18,** 1–8.
37. Niu, Q., Perruzzi, C., Voskas, D., Lawler, J., Dumont, D. J. & Benjamin, L. E. (2004) *Cancer Biol. Ther.* **3**, 402–405.
38. Gory, S., Vernet, M., Laurent, M., Dejana, E., Dalmon, J. & Huber, P. (1999) *Blood* **93,** 184–192.